pH ratiometrically responsive surface enhanced resonance Raman scattering probe for tumor acidic margin delineation and image-guided surgery

Wenjia Duan[a]†, Qi Yue[b]†, Ying Liu[c]†, Yunfei Zhang[a], Qinghua Guo[a], Cong Wang[a], Shujie Yin[a], Dandan Fan[a], Wenjing Xu[c], Jiexian Zhuang[a], Jiachao Gong[d], Xinwei Li[a], Ruimin Huang[e], Liang Chen[b] , Silvio Aime[f], Zhongliang Wang[g] Jianfeng Feng[c], Ying Mao[b], Xiao-Yong Zhang[c]*, and Cong Li[a]**

Abstract: Surgery remains the mainstay for most solid tumor treatment. However, surgeons face challenges in intra-operatively identifying invasive tumor margins due to their infiltrative nature. Incomplete excision usually leads to early recurrence, while aggressive resection may injure adjacent functional tissues. Herein, we reported a pH responsive ratiometric surface-enhanced Raman scattering (SERRS) probe that determined the physiologic pHs with high sensitivity and tissue penetration depth via an innovative mechanism named spatial orientation induced intramolecular energy transfer (SOIET). Due to the positive correlation between tumor acidity and malignancy, an acidic margin-guided surgery strategy was conducted in live animal models by intra-operatively assessing tissue pH/malignancy of the suspicious tissues in tumor cutting edge. This surgery remarkably extended the survival of animal models and minimized their post-surgical complications, showing the promise to precisely identify the invasive tumor boundaries and achieve the balance between maximum tumor debulking and minimal functional impairments.

1. Materials. All chemical reagents, if not specified, were purchased from Adamas Reagent Co. Ltd. and were used without further purification. Silver nitrate, phosphorus oxychloride were purchased from Sinopharm Chemical Reagent, silica gel (200-300 mesh) and cyclohexanone were purchased from Aladdin Reagent. HS-PEG^{5K}-OMe, HS-PEG^{5K}-NHS were purchased from JenKem Technology. The angiopep2 peptide was purchased from Chinapeptides Co. Ltd. Culture media, fetal bovine serum (FBS), trypsin, penicillin and streptomycin were purchased from Thermo-Fisher Scientific Inc. Immune staining blocking buffer, immune staining primary antibody dilution buffer, QuickBlock™ secondary antibody dilution buffer for immunofluorescence and antifade polyvinylpyrrolidone mounting medium were purchased from Beyotime Biotechnology.

2. Instruments. ^{1}H and ^{13}C NMR spectra were recorded on a 400 MHz (Varian, USA) or 600 MHz (Bruker, USA) NMR spectrometer. Confocal fluorescence images were collected on a Zeiss LSM 710 META confocal laser scanning microscope (Carl Zeiss). Fluorescence images were processed by ZEN 2012 software. The fluorescence intensities of the images were quantified by ImageJ software. Hydrodynamic sizes and zeta potentials were acquired by a Malvern Zetasizer ZS90 (Malvern Instruments Ltd., UK). pH dependent absorption and emission spectra were collected by UV-2550 UV−vis spectroscopy (Shimadzu, Japan) and RF-5301PC spectrofluorophotometer (Shimadzu, Japan) respectively. Transmission electron microscopy (TEM) images were obtained using a JEOL 2100F (JEOL, Japan). Ex vivo confocal Raman spectroscopic images were obtained from a Raman confocal microscopic system (XploRA confocal microRaman system). In vivo SERS spectra were recorded using the QE65 Pro handheld Raman scanner (Ocean Optics Inc., USA) with a 785 nm excitation laser. SERS spectra were disposed by LabSpec5 software (v2.02, 2010). Small dorsal kit-SM100 together with the C-clamp used for establishing dorsal skin-fold window chamber model were purchased from APJ Trading Co. (USA). White light images of window chamber model were taken by the stereomicroscope (Fluoca SZ51, China). In vivo MRI studies were conducted using a 11.7 T small animal micro-MRI scanner (Bruker BioSpec, Germany). Microcentrifuge (Thermo scientific, USA), digital dry bath incubato (Labnet, USA) and electrophoresis apparatus trophoresis (BIO-RAD, USA) were used in immunoblotting

studies.

3. Experiments Section

3.1 Synthesis of Raman molecular reporter IR7p.

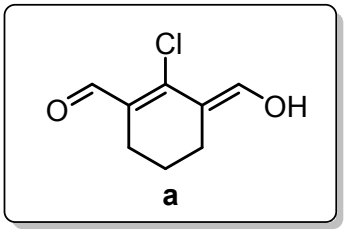

Synthesis of compound **a**. 20 mL *N,N*-dimethylformamide (DMF) (273 mmol, 5.40 eq.) was mixed with 20.0 mL CH_2Cl_2 to obtain solution 1. Meanwhile, 17.5 mL $POCl_3$ (115 mmol, 2.30 eq.) was mixed with 2.5 mL dichloromethane (DCM) to obtain solution 2. Next, solution 2 was added dropwise into solution 1 in an ice bath to obtain solution 3. After 30 min, cyclohexanone (5.0 g, 50.0 mmol, 1.00 eq.) was added into solution 3, followed by stirring for 6 h at 80 °C under reflux. Then the reactive mixture was poured into ice and kept overnight to obtain compound **a** as a yellow solid (8.0 g, yield: 92%).

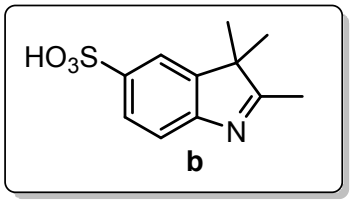

Synthesis of compound **b**. Hydrazinobenzenesulfonic acid (12.9 g, 67.0 mmol) was mixed with 3-methyl-2-butanone (7.00 mL, 67.0 mmol) in acetic acid (30 mL). The solution was refluxed for 4 h and cooled to room temperature. The reactive solid was washed with diethl ether and dried under vacuum to obtain compound **b** as a pink solid (18.0 g, yield: 90%).

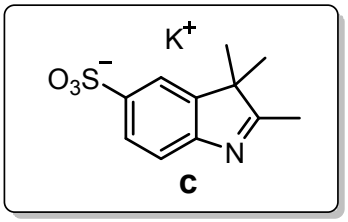

Synthesis of compound **c**. 2,3,3-trimethylindolenine-5-sulfonic acid (18.0 g, 59.0 mmol) was dissolved in 20 mL methanol, to which 2-propanol saturated in potassium hydroxide (300 mL) was added, followed by stirring. The reactive solid was washed with 2-propanol and desiccated under vacuum to obtain potassium salt of compound **c** (15.2 g, yield: 93%).

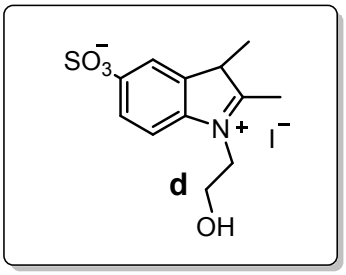

Synthesis of compound **d**. Compound **c** (441 mg, 1.59 mmol) and 2-iodoethanol (950 μL, 12.2 mmol) were dissolved in 15 mL 1,2-dichlorobenzene. The solution was refluxed with vigorous stirring for 48 h

at 100 °C. The resulting solid was washed with 500 mL acetone to obtain compound **d** as a fuchsia solid.

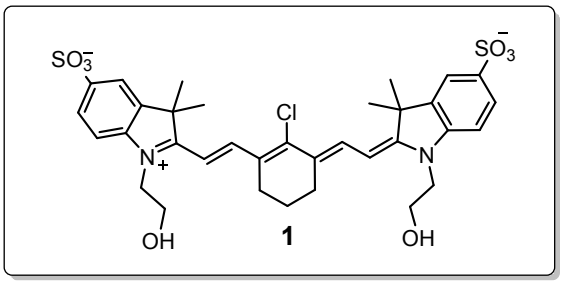

Synthesis of compound **1**. Compound **a** (203 mg, 1.18 mmol) and compound **d** (730 mg, 2.26 mmol) were dissolved in 50 mL mixed solvent ($C_4H_{10}O$:C_3H_6O = 7:3, V:V), and kept it refluxing with stirring under anaerobic condition overnight at 120 °C. Then the product was recrystallized in anhydrous ether after evaporating. Dark green solid was further purified via silica gel chromatography (CH_2Cl_2:CH_3OH =3:1, V:V) to give pure compound **1**. Compound **1** was stored at 4 °C and kept away from light. ^{1}H NMR (400 MHz, DMSO) δ 8.24 (d, *J* = 13.4 Hz, 2H), 7.79 (s, 2H), 7.64 (d, *J* = 6.6 Hz, 2H), 7.39 (s, 2H), 6.43 (d, *J* = 13.6 Hz, 2H), 5.15 (s, 2H), 4.29 (s, 4H), 3.78 (s, 4H), 2.69 (s, 4H), 1.83 (s, 2H), 1.68 (s, 12H). ^{13}C NMR (600 MHz, DMSO) δ 173.76 (s), 147.97 (s), 145.88 (s), 143.02 (d, J = 6.2 Hz), 140.82 (s), 126.61 (d, J = 46.5 Hz), 120.08 (s), 111.38 (s), 103.02 (s), 58.65 (s), 49.39 (s), 47.43 (s), 27.84 (d, J = 16.3 Hz), 26.33 (s), 20.78 (s).

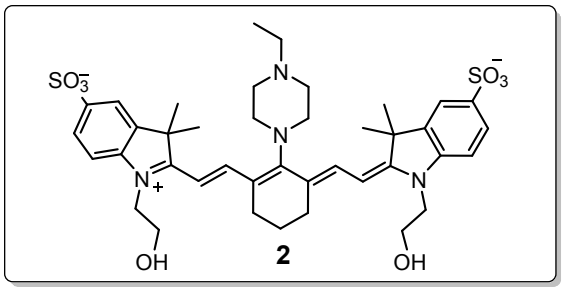

Synthesis of compound **2**. Compound **1** (400 mg, 0.513 mmol) was dissolved in DMSO (20 mL). To this solution was added ethyl piperazine (330 μL, 2.56 mM), followed by stirring for 12 h at 100 °C to afford compound **2** as a royal blue solution. The blue solution was further purified via silica gel chromatography (CH_2Cl_2:CH_3OH = 2.5:1, V:V) to obtain compound **2**.

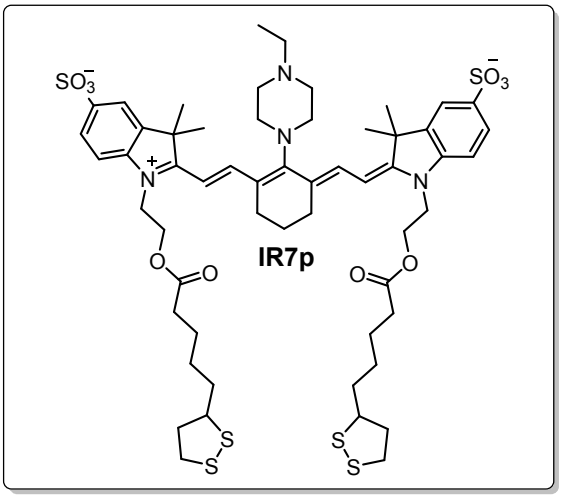

Synthesis of compound **IR7p**. Compound **2** (11.7 mg, 0.0115 mmol) was mixed with DMAP (4.21 mg, 0.0345 mmol), lipoic acid (11.9 mg, 0.0575 mmol) and DCC (5.36 μL, 0.0345 mmol) in DMF (2.00 mL). The reaction was kept in dark for 18 h. The solution was further purified via

silica gel chromatography (CH_2Cl_2:CH_3OH= 5:1, V:V) to give pure **IR7p** as a dark blue solid. ^{1}H NMR (400 MHz, DMSO-d_6) δ 7.58 (d, J = 12.7 Hz, 2H), 7.51 (s, 1H), 7.33 (t, J = 7.1 Hz, 3H), 7.24 (d, J = 7.0 Hz, 2H), 7.12 (d, J = 7.4 Hz, 2H), 6.03 (d, J = 13.5 Hz, 2H), 4.37 (d, J = 25.0 Hz, 10H), 3.78 (s, 4H), 3.13 (ddd, J = 21.3, 13.8, 6.7 Hz, 8H), 2.69 (s, 4H), 2.20 (t, J = 7.1 Hz, 2H), 2.11 (t, J = 7.1 Hz, 5H), 1.81 – 1.73 (m, 5H), 1.62 (d, J = 16.5 Hz, 15 H), 1.50 (s, 5H), 1.42 – 1.29 (m, 12H), 1.24 – 1.16 (m, 6H), 1.10 (s, 2H), 0.84 (d, J = 6.4 Hz, 3H). ^{13}C NMR (600 MHz, DMSO-d_6) δ 174.33 (s), 172.52 (s), 142.68 (s), 139.90 (s), 128.08 (s), 124.74 – 123.49 (m), 123.16 (d, J = 48.6 Hz), 122.12 (s), 109.70 (s), 95.77 (s), 60.31 (s), 56.08 (s), 55.89 (s), 53.76 (s), 51.64 (s), 47.46 (s), 42.00 (s), 38.09 (d, J = 4.4 Hz), 34.02 (d, J = 14.5 Hz), 33.48 (s), 33.25 (s), 30.92 (s), 28.40 (d, J = 15.3 Hz), 28.35 – 27.92 (m), 27.92 – 27.74 (m), 26.32 (s), 24.24 (s), 23.82 (s). TOF-MS calculated for $C_{56}H_{74}N_4O_{10}S_6^+$ [M^+]:1154.3729, found 577.1870.

3.2 Absorption study. The pH dependent absorption spectra of **IR7p** were collected by using UV-2550 UV spectrophotometer (Shimadzu Co). The solutions of **IR7p** (6.0 μM) in disodium hydrogen phosphate-citric acid buffer solutions with pH values in a range of 2.0–8.0 were prepared and 0.5 pH was taken as an interval unit. The scanning speed was 1.0 nm/s and the slit width was 5.0 nm. The scanning wavelength range was from 400 nm to 900 nm.

3.3 Sensitivity study. Disodium hydrogen phosphate-citric acid buffer solution with pH values of 5.5, 6.5, 7.5 and 8.5 were prepared. For each buffered solution with a fixed pH value, **AuS-IR7p** solutions with concentrations of 105, 53, 26, 13, 7.0, 3.0, 2.0, and 1.0 pM were prepared. The SERRS signal intensities of **AuS-IR7p** were determined by quantifying the characteristic Raman peak assigned to ring breathing vibration (~541 cm^{-1}). The incident laser power was 80 mW and the laser wavelength was 785 nm. The confocal Raman spectroscopic images were acquired with a step width of 3.0 μm and an acquisition time of 1.0 s.

3.4 Transmission electron microscopy (TEM) studies. The samples were prepared by dropping 15 μL nanoparticle solution on a copper grid coated with amorphous carbon. The excess liquid was blotted and the grids were air-dried. TEM images and selected area electron diffraction (SAED) pattern were carried out on a JEOL 2100F (JEOL) field emission high-resolution transmission electron microscope with an

accelerating voltage of 200 kV. TEM images were processed with the Digital Micrograph software (Pleasanton).

3.5 Dynamic light scattering (DLS) studies. Hydrodynamic size and zeta potential (ζ-potential) of the gold nanoprobes were analyzed in disposable zeta potential cells using Malvern Zetasizer ZS90 (Malvern Instruments Ltd.) equipped with a 4 mW He-Ne laser. Sample was diluted to 1 pM and suspended before testing. ζ-potential was calculated by the Zetasizer software (Worcestershire) using the Smoluchowski model.

3.6 Tissue penetration depth study. The fresh mouse brain tissues were excised and then fixed in 4% paraformaldehyde (PFA) for 24 h. With the help of micrometer caliper, the fixed brain tissues were cut into slices (0.7 × 0.7 mm) with thicknesses of 0.3, 0.5, 1.0, 1.2, 1.5, 1.8 and 2.2 mm. In a small round dish, 200 μL of **AuS-IR7p** solution (100 pM) was covered with the brain slice with different thicknesses. Raman confocal microscope (XploRA confocal microRaman system) was used to record the Raman spectra. The Raman intensities of **AuS-IR7p** were obtained by quantifying the characteristic twin peak (~541 cm^{-1}). The Raman microscope was equipped with 785 nm laser. The step size was 80 μm and the acquisition time was 1.0 s. The incident laser was applied with a power density of 80 mW.

3.7 In vitro pH value determination. The pH dependent Raman spectra of **IR7p** was collected by using QE65 Pro handheld Raman scanner (Ocean Optics Inc., USA). The solutions of **AuS-IR7p** (100 pM) in buffer solutions with pH values in a range of 2.0–8.0 were prepared. The average pH values in each pixel was determined by quantifying the intensity ratio of selected Peak2 (450−595 cm^{-1}) to Peak1 (280−370 cm^{-1}) followed by substitution into the fitting formula. The incident laser was applied with a power density of 80 mW and the laser spot was focused at the center of solution. The integration time was 1.0 s and accumulation time was 1.0 s. Raman spectra were collected and processed by LabSpec 5 Spectroscopy Suite Software.

3.8 Construction of IDH1R132H mutant lentivirus. The DNA plasmid and lentivirus were designed and constructed by Shanghai GeneChem (Shanghai, China). The vector was Ubi-MCS-3FLAG-CBh-gcGFP-IRES-puromycin. The following primers were used to amplify the sequence: F:5'-

AGGTCGACTCTAGAGGATCCCGCCACCATGTCCAGAAAAAT CCAAGGAGG-3'; R:5'-TCCTTGTAGTCCATACCAAGTTTGGCCTGAGCTAATTTGG-3'. Then, the PCR products were inserted into GV492 plasmid vector. Blank GV492 plasmid vector was used as a control. IDH1 R132H plasmid vectors, packaging plasmids Helper 1.0 and Helper 2.0 were transferred to 293T cells for lentivirus packaging. The harvested lentivirus were concentrated, purified and stored at -80 °C.

3.9 Establishment of orthotopic glioblastoma xenograft in rats. All animal studies were performed in compliance with the guidelines set by Chinese Committee of Management of Laboratory Animals and the overall project protocols were approved by the Ethics Committee of Fudan University. The rat glioblastoma C6 cell line was obtained from Huashan Hospital, Fudan University. Male Sprague Dawley rats (180−200 g) were purchased from Shanghai Slac Lab Animal Ltd (Shanghai, China). In brief, the mice were first anesthetized by 10% chloral hydrate. C6 rat glioblastoma cells (5×10^5 cells in 6 μL PBS) were stereotaxically injected into the right cerebral hemisphere at 4.0 mm to the side of the bregma and 5.0 mm deep into the brain surfaces using a 10 μL Hamilton syringe. The velocity of the injection was 2.0 μL/min and the syringe were left in place for 5 min to avoid reflux after injection. At 7 days post inoculation, GBM model establishment was confirmed by T2W-MRI.

3.10 *In vivo* MRI studies. MRI experiments were performed in a BioSpec 11.7T horizontal scanner with a 75/40 mm diameter quadrature volume coil (Bruker, Ettlingen, Germany). Rat models were kept anesthetized by a gas mixture of isoflurane/oxygen (2%/98%, volume ratio). Bite and ear bars were used to reduce respiration-induced motion artifacts and the respiration and rectal temperature were monitored (SA Instruments, Inc., Stony Brook, NY, USA). For structural analysis, T2W-MR images were acquired using a rapid acquisition with relaxation enhancement (RARE) sequence with the following parameters: repetition time (TR)/echo time (TE) = 3500/10 ms, acquisition matrix = 256×256, NA = 2, field of view (FOV) = 32×32 mm, number of slices = 26, no gap, slice thickness = 0.8 mm, flip angle (FA) = 90°. After surgery, CE-T1W images were acquired after i.v. injection of 0.1 mM Gd^{3+}-DTPA/kg. The parameters for CE-T1W MRI were as followed: TR/TE = 1000/5.5 ms; acquisition matrix = 256×256; NEX = 6; FOV = 32×32 mm; number of slices = 26; slice thickness = 0.8mm, flip angle = 90°.

3.11 Acidic margin-guided glioblastoma resection. Rat models bearing the C6 GBM xenograft were randomly divided into three groups including the metabolic margin, structural margin and white light guided surgery groups. All animal models were anesthetized with 10% (400 μL/100 g) chloral hydrate and fixed on the operation platform. At the beginning of the craniotomy, skull window at the right front parietal region around bregma with a size of 0.8 cm x 0.5 cm was exposed according to the preoperative MR images. A handheld Raman scanner was used to scan the tumor location with a 785 nm excitation laser, a power density of 168 mW and acquisition time of 200 ms. The diameter of the laser spot was in a range of 0.3−0.5 mm when the laser spot was focused at the region of interest. The Raman scanner was connected with a computer that was equipped with Oceanview software. By this way, the Raman spectrum of the region of interest could be simultaneously displayed on the computer screen. For the metabolically acidic margin guided surgery, the average pH values in each pixel was determined by quantifying the intensity ratio of selected Peak2 (450−595 cm^{-1}) to Peak1 (280−370 cm^{-1}) followed by substitution into the fitting formula. Guided by the real-timely generated pH map, acidic region in the tumor bed was excised until no tissue with pH value below 7.0 could be detected under any detection angles of the handheld scanner. For the structural margin guided surgery, the tumor was removed piece-by-piece by monitoring the characteristic twin Raman peak of control probe **AuS-IR7** at 509 and 541 cm^{-1}. For the white light guided surgery, the resection depended on the preoperative MR images and the experience of the surgeon.

3.12 Neurological assessment (NA). The functional testing contents included forelimb and hindlimb flexion tests, visually and contact triggered placing tests, and hindpaw grasping reflex test. Behavioral tests were performed before and at 3, 7, 15 and 30 days post resection by an investigator blinded to the experimental grouping. The tests consisted of a Neuroscore Testing and each step was repeated three times. This experiment was designed to detect functional deficits in specific brain areas. Neurological function evaluation was graded on a scale of 0–21. A score of zero was normal. The higher the score, the more severe the injury was.

3.13 Statistics. Statistical analysis was performed using Origin 9.1 software (Microcal Software Inc., Northampton, USA), MATLAB (R2018a) and GraphPad Prism 7.00. Data are presented as the mean ± S.D. or mean ± SEM for all results. The significance of acidosis related proteins expression was determined by two-tailed t-test and others were calculated via one-way analysis of variance (ANOVA) with a Tukey post-hoc test for multiple comparisons. Survival was analyzed using Kaplan–Meier survival curves. The curves were compared with the log-rank Mantel–Cox test. Probability value (*p*-value) less than 0.05 was considered significant.

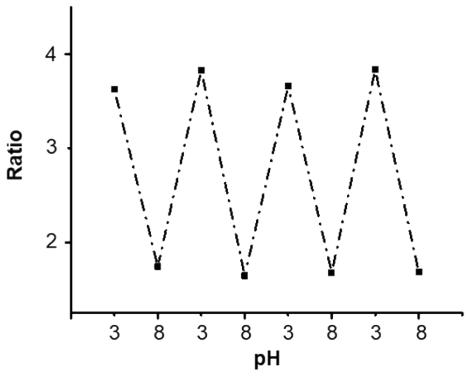

Figure S1. AuS-IR7p shows reversible pH responsive ability. The initial concentration was 100 pM. Laser power: 80 mW. Acquirement time: 1.0 s.

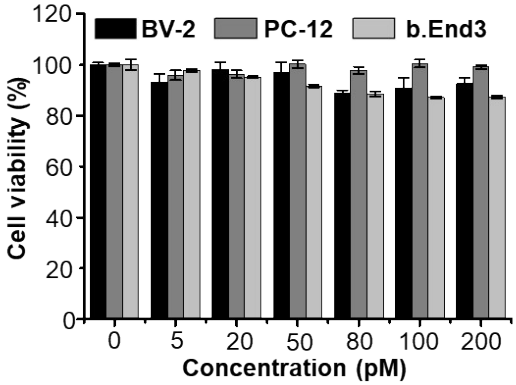

Figure S2. AuS-IR7p shows minimized cytotoxicity. Viabilities of BV-2 (A), PC-12 (B) and bEnd3 cells (C) after treatment of **AuS-IR7p** for 48 h with concentrations ranged from 0 to 200 pM. Cell viabilities were determined by CCK-8 assay. Data are presented as the mean ± s.d. for three replicates.

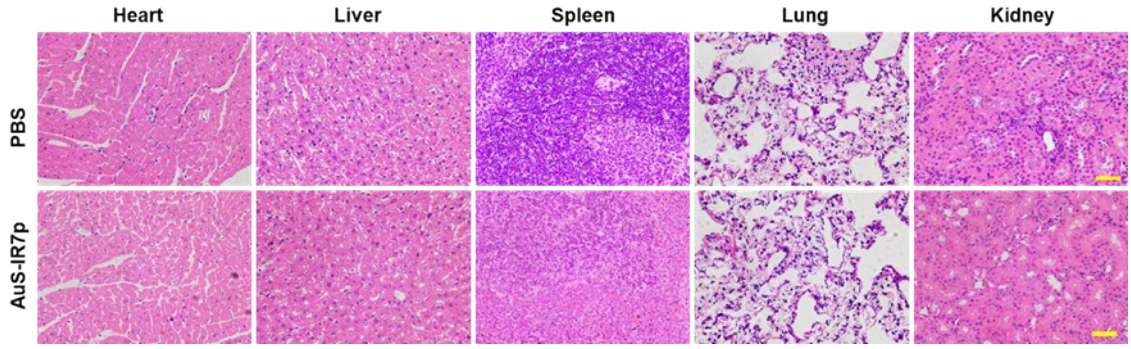

Figure S3. AuS-IR7p shows minimized toxicity to the major organs in Rats. H&E staining of major organs (heart, liver, spleen, lung, kidney, brain) from healthy mice treated with PBS or AuS-IR7p (1.5 μmol/100g). The organs were harvested at 14 days after PBS or AuS-IR7p administration. No obvious abnormities or lesions were observed. Scale bar: 50 μm.

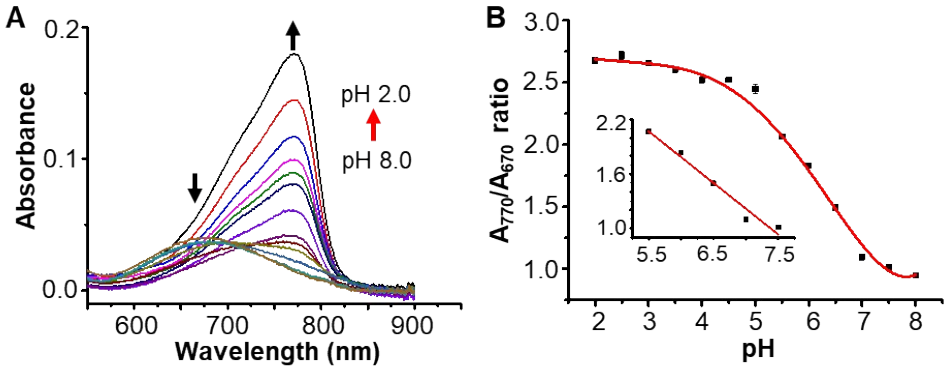

Figure S4. (A) pH-dependent absorption of **IR7p**. The pH changed with an interval of 0.5 units. (B) Plotting absorption ratio (A_{750}/A_{670}) of **IR7p** as a function of pH. The inset shows measurements in the linear response region.

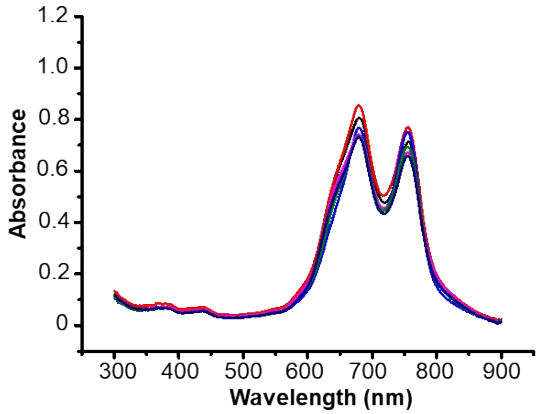

Figure S5. Absorption spectra of **IR7** (4 μM) in buffered solutions with different pHs (pH 3.0–8.0). pH changed with an interval of 1.0 units.

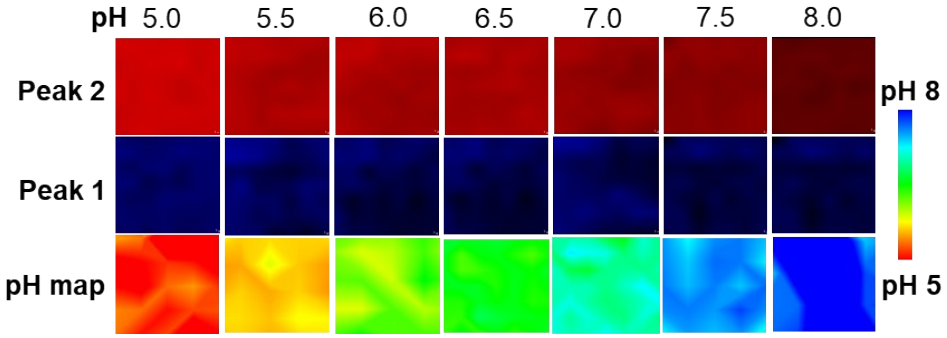

Figure S6. Integrated Raman intensity images of Peak 2 or Peak 1 in buffered solutions with presence of **AuS-IR7p** (1 nM). Corresponding pixel to pixel pH maps of the buffered solutions were generated by comparing the Peak2/Peak2 Raman intensity ratio against the calibration curve.

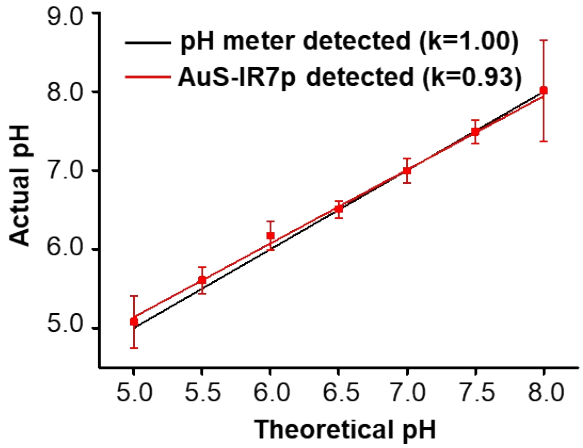

Figure S7. pH values determined by **AuS-IR7p** (100 pM) coincide well with the values measured by pH meter. Data are presented as the mean ± S.D. (n=3).

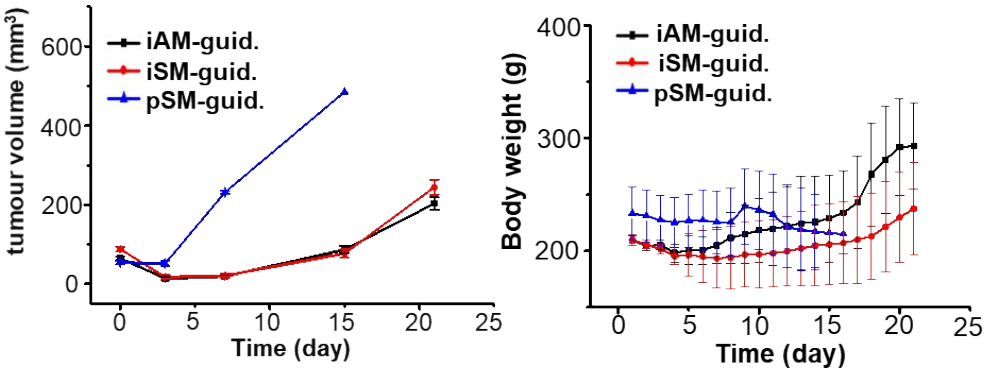

Figure S8. Time dependent tumor volume and body weights curve post-surgery.

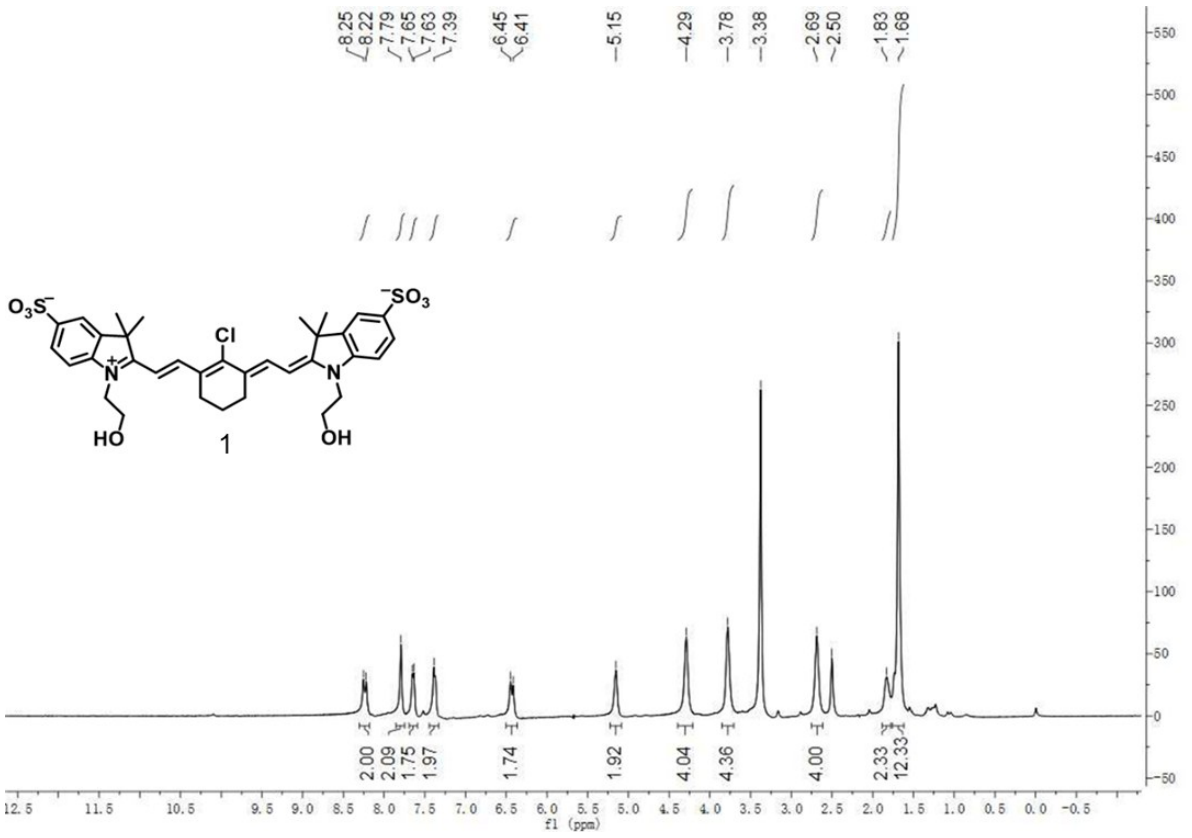

Figure S9. ^{1}H NMR spectrum of compound 1 in DMSO-d_6.

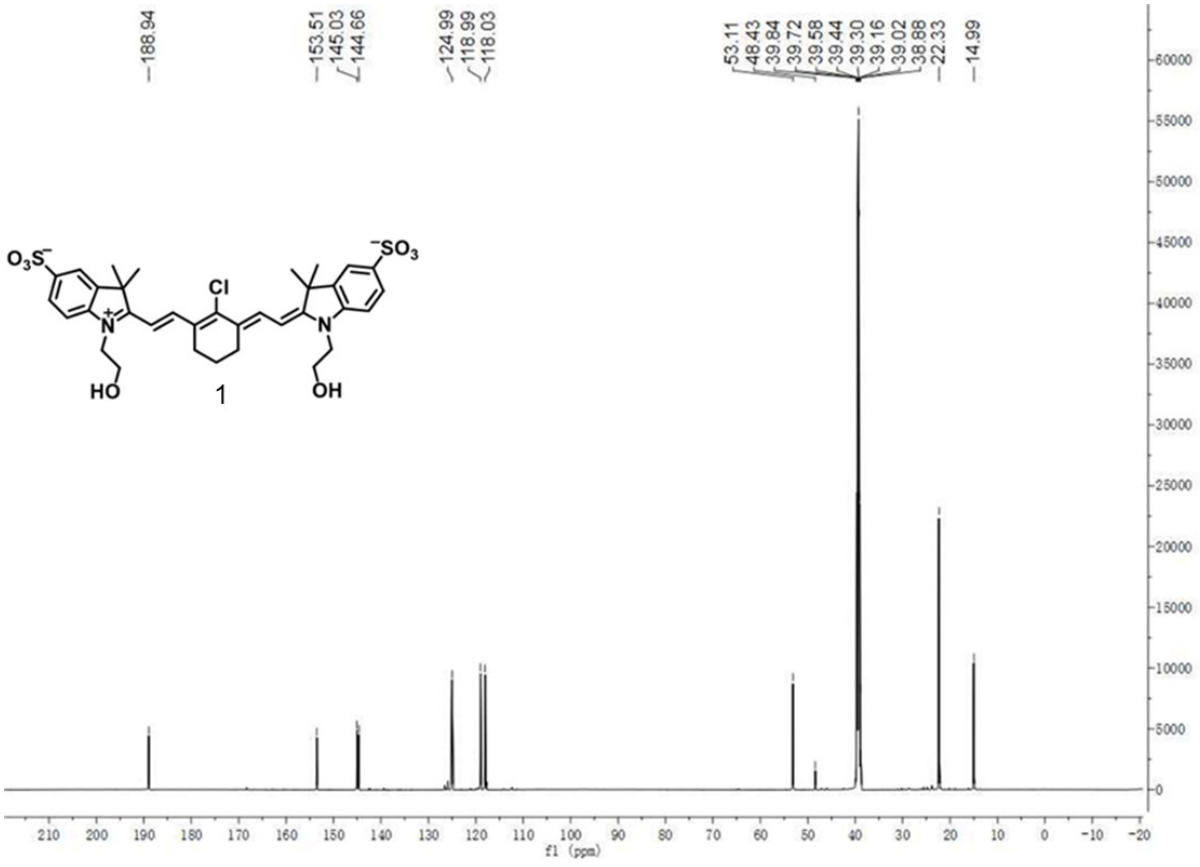

Figure S10. ^{13}C NMR spectrum of compound 1 in DMSO-d_6.

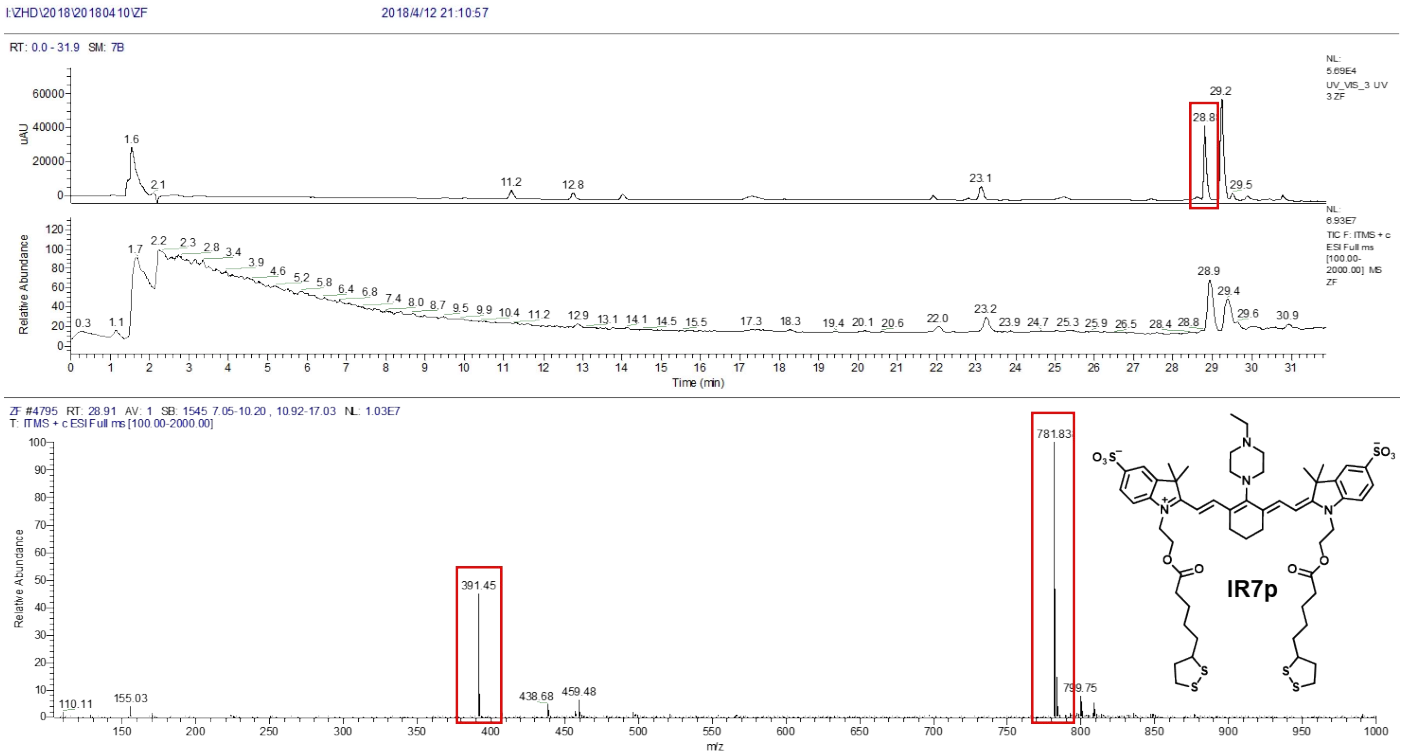

Figure S11. MS spectrum (ESI) of **IR7p**.

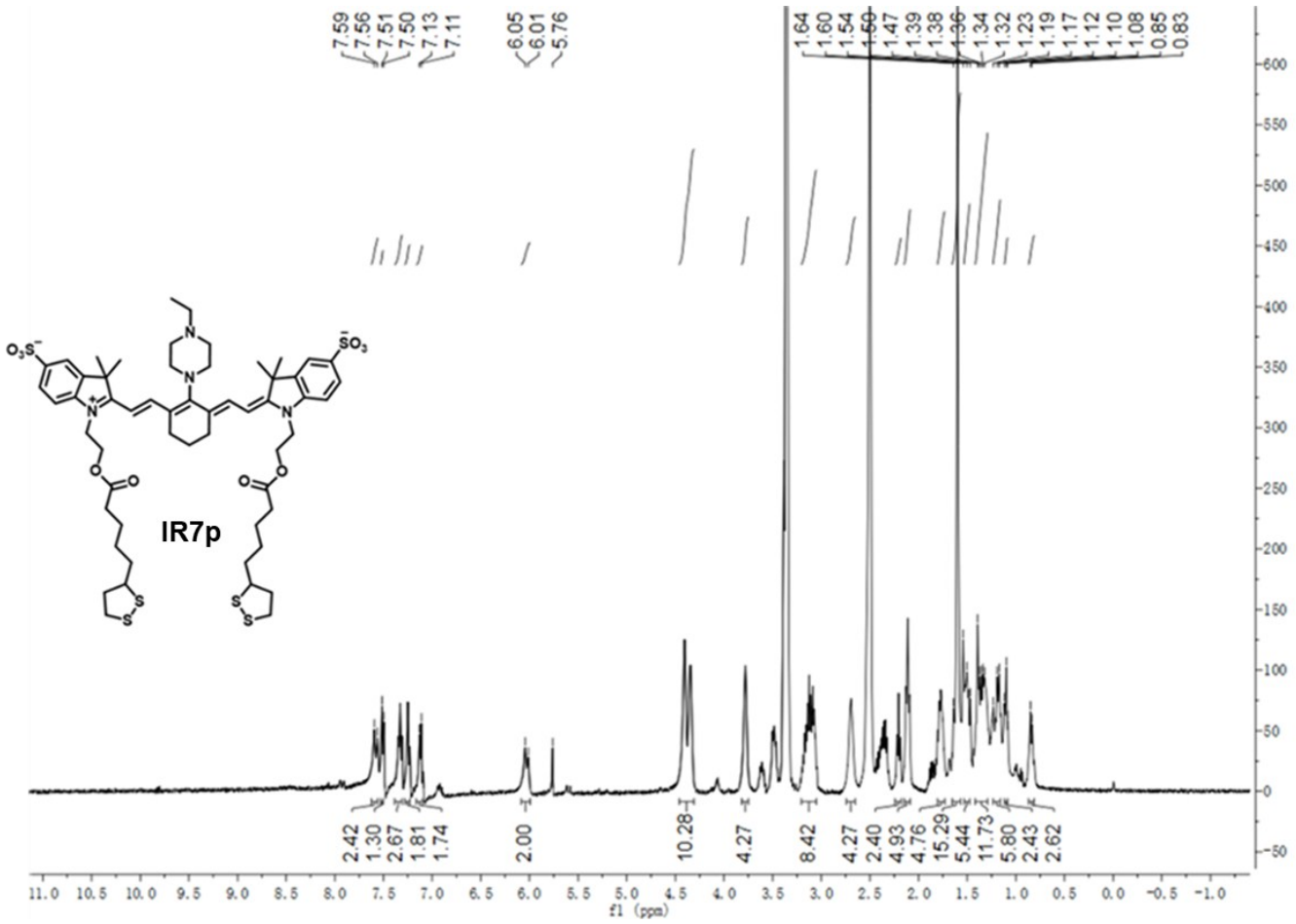

Figure S12. ^{1}H NMR spectrum of **IR7p** in DMSO-d_6.

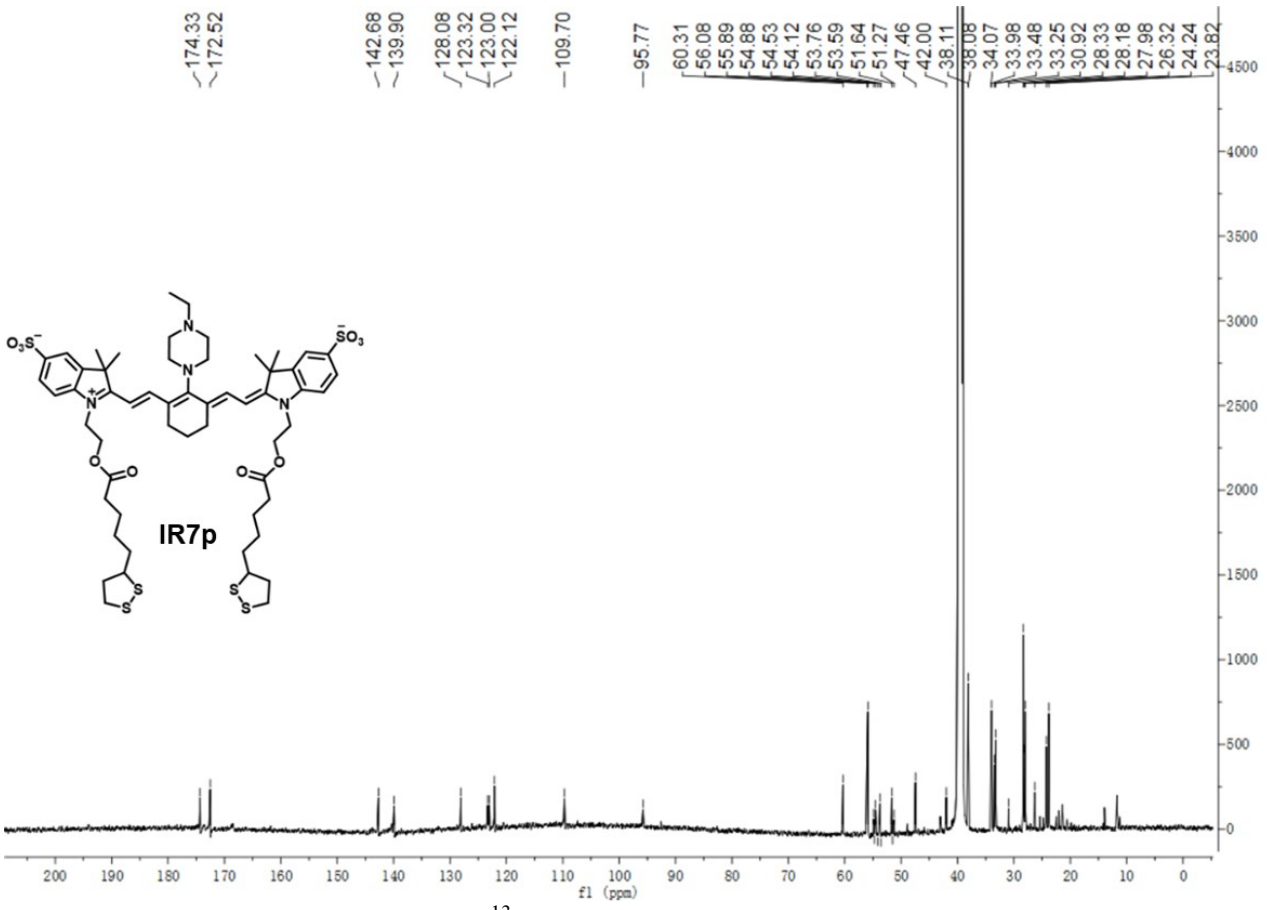

Figure S13. ^{13}CNMR spectrum of **IR7p** in DMSO-d_6.

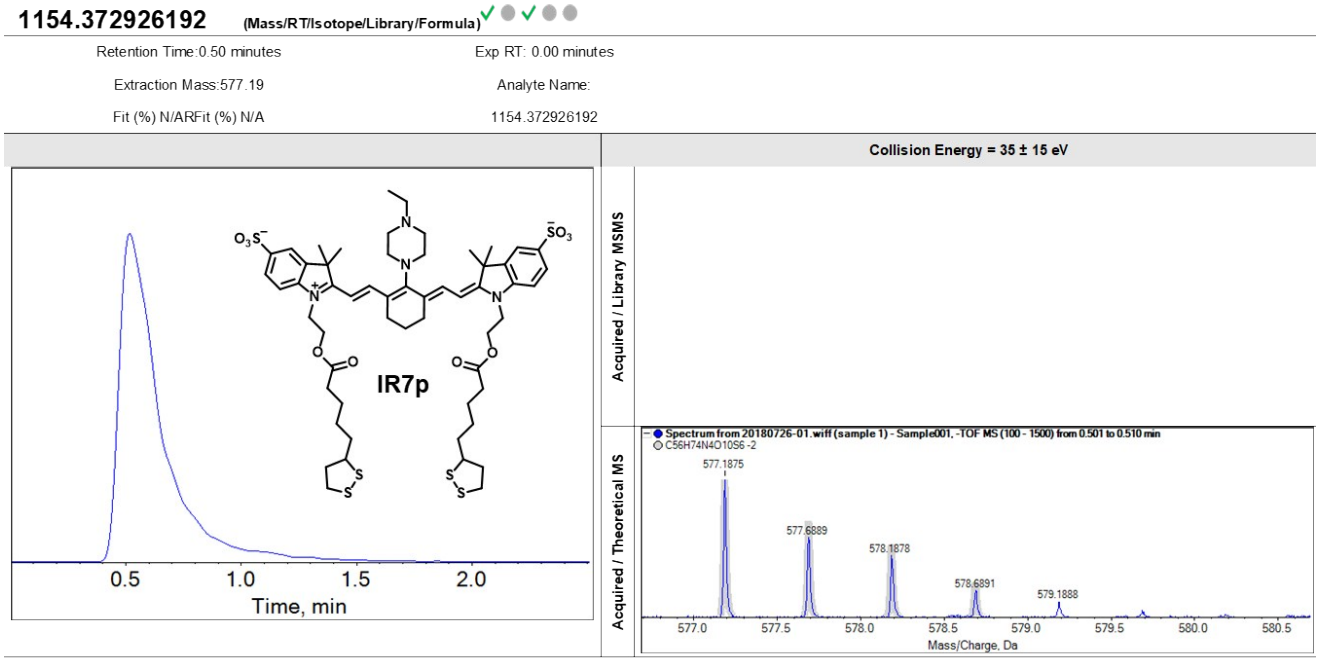

	Compound Name (Library Hit)	Score	Formula	Intensity	Threshold	Expected m/z	Found at m/z	Error (ppm)	Expected RT (min)	Found RT (min)	RT Delta (min)	Isotope Diff (%)	Library Score(%)
✓●✓●●	1154.372926192(Final)	68%	C56H74N4O10S6	31626	50	577.1870	577.1875	0.9	0.00	0.50	0.50	11.9%	N/A

Figure S14. UPLC-Q-TOF-MS/MS spectrum (ESI) of **IR7p**.